Dual-Wavelength Linearization of Optically Phase-Modulated Analog Microwave Signals

Bryan M. Haas, *Member, IEEE*, Vincent J. Urick, *Member, IEEE*, Jason D. McKinney, *Member, IEEE, Member, OSA*, and Thomas E. Murphy, *Senior Member, IEEE, Member, OSA*

***Abstract*—We demonstrate a new technique for improving the linearity of a microwave photonic signal transmission link. The method employs a single conventional lithium-niobate phase modulator at the transmitter, with two different C-band optical wavelengths that are polarized along orthogonal axes of the modulator. The spurious-free dynamic range is shown to improve by 15 dB compared to a single-wavelength unlinearized system. Unlike earlier schemes that require continuous control and adjustment at the transmitter in order to maintain linearity, the new method enables all of the linearization to be controlled at the receiver end.**

***Index Terms*—Analog optical links, microwave photonics intermodulation distortion, phase modulation, polarization.**

I. Introduction

RECENT improvements in $LiNbO_3$ modulator and photodetector technologies have renewed interest in high-performance radio-over-fiber applications using external electrooptic modulators [1]–[3]. However, the spurious-free dynamic range (SFDR) of these links is still limited by the in-band third-order intermodulation distortion (IMD) products caused by the nonlinear transfer function of the Mach–Zehnder modulator (MZM) [4].

Phase-modulated links offer several advantages in comparison to MZM-based links for transmitting analog radio signals over fiber [5], [6]. Although they too exhibit third-order IMD as a result of the detection process [7]–[9], the benefits of optical phase modulation can make it an attractive alternative. Phase modulators require no biasing or other external control at the modulator, which improves the reliability, simplicity, size, weight, and power of the transmitter. This can be an important advantage in antenna remoting applications. The constant optical power within the fiber can mitigate the effects of crosstalk [10], which is advantageous if the link is multiplexed in a single fiber with other wavelength channels.

Despite these advantages, comparatively little work has been done to develop linearized phase-modulated analog links. One reason is that phase-modulated links generally require a more complex receiver architecture. In an antenna remoting scenario, however, the receiver is in a protected environment, and one is often willing to accept a more complex receiver in order to simplify the transmitter. The receiver architecture for the phase-modulated system described here can utilize balanced detection to suppress common-mode intensity noise, without necessitating a dual-fiber run from the modulator as is necessary for a MZM-based link.

Here, we present a technique to linearize the phase-modulated signal so the suboctave instantaneous bandwidth SFDR is limited not by third-order, but by the smaller fifth-order terms of the IMD products. The link presented here uses a technique similar in concept to [11]–[14] in order to linearize the recovered microwave signal by suppressing the third-order term of the IMD, but adapts the technique for use in a phase-modulated link.

II. Theory

Fig. 1 depicts the setup used to demonstrate linearized electrooptic phase modulation. As in an earlier scheme, the method makes use of the fact that in lithium niobate, as in many other electrooptic materials, the electrooptic coefficient is different for the two polarization states [13]–[16]. When two different optical wavelengths are launched along the TE and TM axes of the phase modulator, as in Fig. 1, they are each modulated by different amounts. The two wavelengths are demultiplexed at the receiver and each one is separately demodulated in an asymmetric-delay Mach–Zehnder interferometer (MZI) with balanced photoreceivers [8]. When properly biased, the MZI converts phase modulation into intensity modulation, providing a simpler receiver architecture than the heterodyne system reported in [15], [16]. The demodulated microwave signals are then subtracted using a 180°-hybrid coupler. Linearization is achieved by adjusting the relative intensities of the two wavelengths in a way that cancels out the third-order intermodulation distortion.

The optical field in the upper (TM) path of the receiver immediately before the MZI is described by a phase-modulated optical carrier

$$u_A(t) = \sqrt{P_A}e^{j\omega_0 t}e^{j\phi_A(t)} \tag{1}$$

where P_A denotes the optical power in the TM channel, ω_A is the optical carrier frequency, and $\phi_A(t)$ represents the phase modulation that is imposed on the TM polarized signal. To simplify the analysis, we have chosen to normalize the optical field so that $|u_A|^2$ represents the total optical power.

Manuscript received January 30, 2008; revised April 16, 2008. Current version published October 10, 2008.

B. M. Haas is with the Laboratory for Physical Sciences, College Park, MD 20740 USA (e-mail: bmhaas@lps.umd.edu).

V. J. Urick and J. D. McKinney are with the U.S. Naval Research Laboratory, Washington, DC 20735 USA (e-mail: vurick@ccs.nrl.navy.mil; jdm@ccs.nrl.navy.mil).

T. E. Murphy is with the Department of Electrical and Computer Engineering at the University of Maryland, College Park, MD 20742 USA (e-mail: tem@umd.edu).

Color versions of one or more of the figures in this paper are available online at http://ieeexplore.ieee.org.

Digital Object Identifier 10.1109/JLT.2008.925656

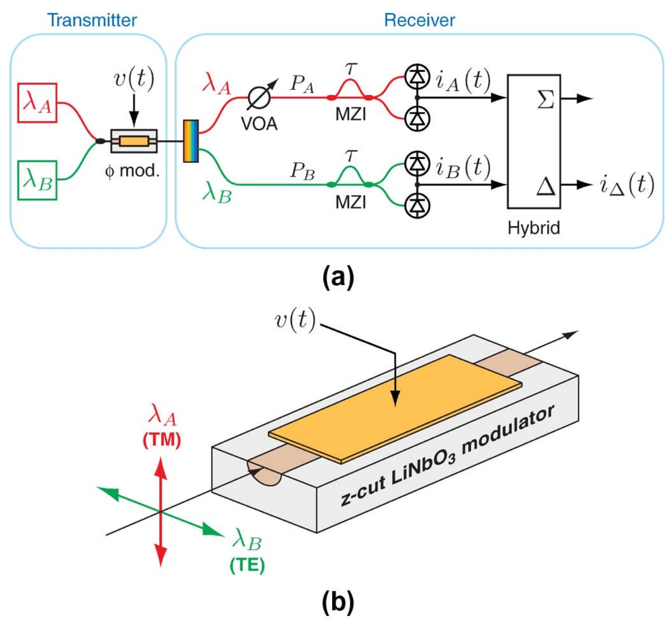

Fig. 1. (a) Schematic diagram of dual-wavelength linearized phase modulated link. (b) The two wavelengths λ_A and λ_B are combined in a polarization-maintaining coupler, and launched along the TM and TE polarization axes of the modulator, respectively.

After passing through the asymmetric MZI, the differential photocurrent $i_A(t)$ at the output of the balanced detector is calculated to be [9]

$$i_A(t) = -\mathcal{R}P_A \cos\left[\phi_A(t-\tau) - \phi_A(t) - \phi_0\right] \qquad (2)$$

where $\mathcal{R}$ is the responsivity of the photodiodes, τ represents group-delay difference between the two arms of the Mach–Zehnder interferometer, and ϕ_0 is the net optical phase difference between the two arms, evaluated at the carrier frequency ω_A. If the interferometer is biased at quadrature, such that $\phi_0 = -\pi/2$, this relationship simplifies to

$$i_A(t) = \mathcal{R}P_A \sin\left[\phi_A(t) - \phi_A(t-\tau)\right]. \qquad (3)$$

Quadrature biasing ensures that the average dc photocurrents in the two detectors remain balanced and equal to $\mathcal{R}P_A/2$. Biasing away from quadrature will not prevent suppression of the third-order IMD term [17], but does lessen the suppression of common-mode noise and, for an intensity-noise dominated link, may decrease SFDR as a result of the elevated noise floor. Nonquadrature biasing also gives rise to even-order distortions that can limit useful application of this technique to suboctave signals.

We now assume that the phase modulator is driven by a sinusoidal microwave tone with frequency Ω

$$v(t) = V_0 \cos\Omega t. \qquad (4)$$

Given this driving signal, the electrooptic modulator imposes a phase modulation of

$$\phi_A(t) = m\cos\Omega t, \quad m \equiv \pi\frac{V_0}{V_\pi^{(\mathrm{TM})}} \qquad (5)$$

where m denotes the phase modulation depth (in radians) and $V_\pi^{(\mathrm{TM})}$ is the half-wave voltage for the TM-polarization.

Optimal receiver performance is obtained by choosing $\tau = \pi/\Omega$ [8], in which case the differential photocurrent evaluates to

$$i_A(t) = \mathcal{R}P_A \sin(2m\cos\Omega t). \qquad (6)$$

The TE-polarized wave (λ_B) experiences a similar phase modulation, but the modulation depth is reduced by a factor of γ compared to the TM case

$$\phi_B(t) = \gamma m\cos\Omega t, \quad \gamma \equiv \frac{V_\pi^{(\mathrm{TM})}}{V_\pi^{(\mathrm{TE})}}. \qquad (7)$$

For $LiNbO_3$ as well as for many poled electrooptic polymers, we expect

$$\gamma = \frac{r_{13}}{r_{33}} \simeq \frac{1}{3}. \qquad (8)$$

The differential photocurrent for the TE-polarized channel is then

$$i_B(t) = \mathcal{R}P_B \sin(2\gamma m\cos\Omega t) \qquad (9)$$

where we have assumed that the TE-receiver is also biased at quadrature and configured so that $\tau = \pi/\Omega$.

The 180° microwave hybrid produces an output signal proportional to the difference $i_A - i_B$

$$\begin{aligned} i_\Delta(t) &= \frac{i_A(t) - i_B(t)}{\sqrt{2}} && (10)\\ &= \frac{\mathcal{R}}{\sqrt{2}}\left[P_A\sin(2m\cos\Omega t) - P_B\sin(2\gamma m\cos\Omega t)\right]. && (11)\end{aligned}$$

By applying the Bessel function expansion

$$\sin(z\cos\theta) = 2J_1(z)\cos\theta - 2J_3(z)\cos 3\theta + \ldots \qquad (12)$$

the component of the output photocurrent at the modulation frequency Ω is found to be

$$i_\Delta = \sqrt{2}\mathcal{R}\left[P_A J_1(2m) - P_B J_1(2\gamma m)\right]\cos\Omega t + \ldots. \qquad (13)$$

Performing a power series expansion of $J_1(2m)$, retaining terms up to third order in m, one finds

$$i_\Delta = \sqrt{2}\mathcal{R}\left[m(P_A - \gamma P_B) + \frac{m^3}{2}(P_A - \gamma^3 P_B)\right]\cos\Omega t + \ldots. \tag{14}$$

The nonlinear terms proportional to m^3 can be eliminated by adjusting the optical powers P_A and P_B so that

$$P_A = \gamma^3 P_B \tag{15}$$

in which case the leading nonlinear terms are proportional to m^5 [12], [13], [18]. As with any method that depends on canceling nonlinear terms, successful suppression of the third-order term is dependent upon precise control of the ratio of optical powers. Small deviations from the ideal ratio decrease the amount of suppression very quickly [19]. The linearization method presented here is notable in that this ratio can be controlled at the receiver rather than the transmitter.

The linearized output photocurrent is then given by

$$i_\Delta = -2\sqrt{2} I_B \gamma(1-\gamma^2) m \cos\Omega t + \ldots \tag{16}$$

where $I_B \equiv \mathcal{R}P_B/2$ is the average dc photocurrent for each of the photodiodes in the TE receiver. We note that when linearized according to (15), the optical power in the TM path is always smaller than the TE power. Therefore, the link gain is in practice limited by I_B, the maximum dc photocurrent that can be sustained in the TE-channel photoreceivers.

Assuming the output current $i_\Delta(t)$ is applied through an impedance of Z_{out} and the input impedance of the modulator is Z_{in}, the net RF power gain of the linearized RF link is calculated to be

$$G_{\text{lin}} = 8\pi^2 \left(\frac{I_B}{V_\pi}\right)^2 \gamma^2(1-\gamma^2)^2 Z_{\text{in}} Z_{\text{out}}. \tag{17}$$

This result should be compared to the non-linearized case, in which all of the light is launched along the TM polarization. In this case, $P_B = 0$, and RF power gain is found to be [9]

$$G_{\text{TM}} = 8\pi^2 \left(\frac{I_A}{V_\pi}\right)^2 Z_{\text{in}} Z_{\text{out}}. \tag{18}$$

For the nonlinearized case, the attainable RF power gain is limited by I_A, the maximum sustainable photocurrent in the TM-channel photodiodes. To simplify the comparison with experiment we have retained the 180° hybrid in the TM-only calculation, although removing this component could yield a 3-dB increase in gain for the nonlinearized case. It should also be noted that the calculations here assume the photodiodes are not internally terminated; internal 50-Ω termination decreases the gain by a factor of 1/4.

The attainable link gain for the linearized case is reduced by the factor of $\gamma^2(1-\gamma^2)^2$ compared to the linearized case, which evaluates to 10.5-dB reduction when $\gamma = 1/3$. This penalty could be reduced to 8.3 dB for the optimal case of $\gamma = \sqrt{1/3}$. Despite this penalty, the linearized system offers suppression of the dominant third-order nonlinear distortion, which significantly improves the dynamic range of the link.

The preceding analysis can be extended to the case when the input signal is comprised of two closely spaced RF tones

$$v(t) = V_0\cos(\Omega_1 t) + V_0\cos(\Omega_2 t). \tag{19}$$

In addition to Ω_1 and Ω_2, the output current i_Δ will contain intermodulation terms at the frequencies $2\Omega_1 - \Omega_2$ and $2\Omega_2 - \Omega_1$. By applying standard Bessel-series expansions, i_Δ is found, after some algebraic manipulation, to be

$$\begin{aligned} i_\Delta(t) = {} & \sqrt{2}\mathcal{R}\,[P_A J_1(2m)J_0(2m) \\ & \quad - P_B J_1(2\gamma m)J_0(2\gamma m)]\cos\Omega_1 t \\ & - \sqrt{2}\mathcal{R}\,[P_A J_2(2m)J_1(2m) \\ & \quad - P_B J_2(2\gamma m)J_1(2\gamma m)]\cos(2\Omega_1 - \Omega_2)t \\ & + \text{similar terms at } \Omega_2 \text{ and } 2\Omega_2 - \Omega_1 \end{aligned} \tag{20}$$

where we define $m \equiv \pi V_0/V_\pi^{(\text{TM})}$, just as in the single-tone case.

In the limit of small m, the Bessel functions can be Taylor-series expanded to give

$$\begin{aligned} i_\Delta(t) = {} & \sqrt{2}\mathcal{R}m(P_A - \gamma P_B)\cos\Omega_1 t \\ & - \sqrt{2}\mathcal{R}\left[\frac{m^3}{2}(P_A - \gamma^3 P_B) \right. \\ & \left. \quad - \frac{5m^5}{12}(P_A - \gamma^5 P_B)\right]\cos(2\Omega_1 - \Omega_2)t \\ & + \text{similar terms at } \Omega_2 \text{ and } 2\Omega_2 - \Omega_1. \end{aligned} \tag{21}$$

When the linearization condition (15) is met, the output photocurrent simplifies to

$$\begin{aligned} i_\Delta(t) = {} & -2\sqrt{2} I_B \gamma(1-\gamma^2) m \cos\Omega t \\ & + \frac{5\sqrt{2}}{6} I_B \gamma^3 (1-\gamma^2) m^5 \cos(2\Omega_1 - \Omega_2)t + \ldots \end{aligned} \tag{22}$$

where $I_B \equiv \mathcal{R}P_B/2$, as before. The intermodulation amplitude grows in proportion to m^5, as expected for a system limited by fifth-order distortion. The fifth-order intercept point is obtained by equating the extrapolated fundamental and intermodulation amplitudes, which gives

$$m_{\text{IIP5}} = \left(\frac{12}{5\gamma^2}\right)^{1/4} \tag{23}$$

which corresponds to an input RF power of

$$P_{\text{IIP5}} = \frac{1}{\pi^2}\left(\frac{V_\pi^2}{Z_{\text{in}}}\right)\sqrt{\frac{3}{5}}\frac{1}{\gamma} \tag{24}$$

per tone.

For a system limited by fifth order intermodulation distortion, the spurious-free dynamic range (SFDR) is calculated to be

$$\mathrm{SFDR}_5 = \left(\frac{G_{\mathrm{lin}} P_{\mathrm{IIP5}}}{S_0 B}\right)^{4/5} \tag{25}$$

where S_0 is the power spectral density of output noise, B is the receiver bandwidth, and G_{lin} is the linearized gain given in (17).

For the nonlinearized (TM-only) system, the intermodulation amplitudes grow in proportion to m^3, and becomes equal in magnitude to the fundamental amplitude when $m = \sqrt{2}$. The corresponding input-referenced third-order intercept point is

$$P_{\mathrm{IIP3}} = \frac{1}{\pi^2}\left(\frac{V_\pi^2}{Z_{\mathrm{in}}}\right) \tag{26}$$

and the third-order limited SFDR is

$$\mathrm{SFDR}_3 = \left(\frac{G_{\mathrm{TM}} P_{\mathrm{IIP3}}}{S_0 B}\right)^{2/3} \tag{27}$$

where G_{TM} is the nonlinearized gain given in (18).

III. Experiment

Two 20-mW telecom-grade distributed feedback (DFB) lasers with linewidths of approximately 2 MHz were used as sources for the link, and amplified with polarization-maintaining erbium-doped fiber amplifiers having an optical noise figure of 4.5 dB. One wavelength ($\lambda_A = 1554.94$ nm) was launched conventionally into the slow axis of a polarization-maintaining fiber (PMF), which was coupled to the vertical, or TM, axis of the optical phase modulator. The other wavelength ($\lambda_B = 1552.52$ nm) was launched into the fast axis of a PMF via a 90° splice, polarization multiplexed with λ_A in a PM coupler, and ultimately fed into the horizontal (TE) axis of the modulator, as depicted in Fig. 1(b). Thus, each axis of the modulator was illuminated with a different wavelength, with >24 dB of isolation measured between the axes at the modulator input. The modulator output consisted then of two wavelengths, each modulated to a different depth owing to the anisotropic electrooptic coefficients for the z and x axes of $LiNbO_3$.

There is no specific amount of polarization isolation or spectral isolation required to achieve suppression of the third-order distortion. Suppression is dependent on the existence of two different modulator transfer functions; any difference will allow suppression to occur, albeit with different gain. Imperfect isolation between the two wavelength or polarization states in the system modifies the effective value of γ and can be compensated by adjusting the power splitting ratio at the receiver per (15), with a change in SFDR in accordance with (17), (24), and (25).

The modulator was a commercial z-cut, Ti-indiffused $LiNbO_3$ phase modulator with PMF input pigtail and SMF output pigtail, and a V_π of 3.25 V at 5 GHz for the TM polarization. Nominally, the V_π for the TE axis should be approximately three times larger, but was experimentally measured to be approximately 4.25 times larger ($\gamma = 1/4.25$) in this device. We believe that the lower than expected modulation efficiency for TE polarization may be a result of increased TE mode size within the Ti-diffused waveguide, resulting in a lower overlap between the RF and optical fields.

At the receiver, the wavelengths were separated in a commercial WDM demultiplexer. Variable optical attenuators (VOAs) were used on each wavelength prior to the demodulation to achieve the desired ratio of photocurrents dictated by (15).

Two asymmetric-delay MZIs were used to convert phase to intensity modulation in the receiver. The MZIs here were thermally-tuned all-fiber devices with a 100-ps relative group delay between the arms. Both MZIs were thermally biased at quadrature and the two complementary outputs were detected through a balanced photodiode pair. The output RF signals were combined in antiphase by the Δ output of the RF hybrid. Equivalently, the MZIs could be set to opposite bias points and the summation output of a hybrid could be used. The photodetectors were identical balanced detectors with internal 50-Ω resistors and a 1-dB compression current of 7-mA per diode.

As detailed in [9], the MZI has a periodic transmission function, which limits microwave frequency range over which it can be used to demodulate the signal. For the 100-ps MZI biased at quadrature, the optimal modulation frequency is approximately 5 GHz in order to satisfy the condition $\Omega\tau = \pi$.

The group delays of the optical paths to each detector were matched to within 2 ps for optimal differential detection and common-mode RIN suppression at each wavelength. The RF output from each balanced detector through the Δ port of the hybrid was balanced to within five degrees of 180° for IMD suppression. Equalizing the delays in this way can also compensate for the birefringent group delay difference between the TE and TM polarization states in the electrooptic modulator, which could become significant at higher frequencies and for longer device lengths.

This provides a relatively simple receiver architecture in comparison to a heterodyne receiver [15]. An important feature of this receiver architecture is that the relative powers of the TE and TM polarizations can be adjusted at the receiver in order to achieve and maintain linearization, with no additional control or complexity at the transmitter. Unlike in earlier approaches, in which a single input wavelength was polarized at an oblique angle to the modulator axes [15], the approach reported here uses an input PM fiber that is co-aligned with the waveguide. Moreover, the dual-wavelength scheme greatly facilitates separation of the two polarization states at the receiver and allows standard single-mode fiber (SMF) to be used between the modulator and receiver.

IV. Results

Results from two-tone testing with tones at 4.7 and 4.9 GHz are shown in Fig. 2. The squares are the measured fundamental tone and IMD powers for TM modulation only, at a dc photocurrent of 6 mA per detector. For this measurement, the TE wavelength was fully attenuated at the receiver.

Similarly, the circles show the measured results when the link is linearized. For this setup, the TE wavelength's power was adjusted to give 6 mA of dc photocurrent per diode, and the

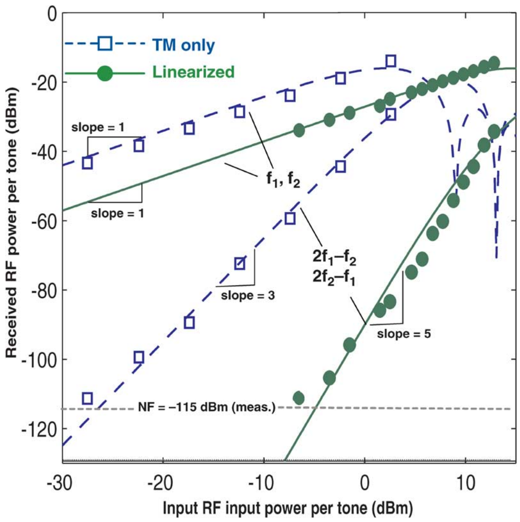

Fig. 2. Plot of measured and calculated signal and IMD powers for TM-only (blue squares) and linearized (green circles) configurations, showing third-order suppression. The fundamental tones are 4.7 and 4.9 GHz. The solid lines indicate calculated curves, adjusted for the experimentally determined electrooptic ratio γ excess RF loss. All measurements were performed using a resolution bandwidth of 10 kHz.

TM optical power was attenuated until the IMD measurements varied with a slope of five on a log–log plot, indicating fifth-order limited performance. Had the modulator's γ been 1/3, the TM optical power should have been the expected 13 dB below the TE power. Because of the different γ, however (determined earlier to be 1/4.25), the actual TM optical power was 18 dB below the TE power. Additionally, the RF gain was measured to be 12.5 dB below the TM-only measurement, in contrast to the expected 10.5 dB.

The output noise power spectral density was measured to be -155 dBm/Hz, and primarily limited by phase-to-intensity noise conversion of the source lasers and EFDA ASE in the MZIs [7], [9]. The balanced detectors suppress the intensity component of common-mode noise but the MZIs expose the phase component [20], which cannot be suppressed by balanced detection. Narrower linewidth source lasers, as demonstrated in [9], could reduce the phase-to-intensity noise.

When the experimentally determined γ of 1/4.25 and approximately 6 dB of excess RF loss are accounted for, the measured data are in good agreement with the calculated predictions from (17) and (25).

Table I summarizes the measured and calculated performance metrics in columns 1 and 2, respectively, for both TM-only and linearized configurations. The measured improvement in SFDR due to suppression of the third-order term in the IMD was 15 dB, in agreement with theory when the 6 dB excess loss is taken into account. The measurement bandwidth was 10 kHz, although the SFDR has been normalized to a 1-Hz bandwidth for ease of comparison to other links.

From Fig. 2, one can see that despite the penalty in net link gain, the dynamic range of the linearized system always exceeds that of the conventional system. In the linearized case, the intermodulation products exhibit a fifth-order dependence on the input power, and therefore the improvement in SFDR over the third-order case decreases with increasing noise bandwidth. For the experiments reported here, the SFDR improvements for 1-MHz and 100-MHz noise bandwidths were 7 and 4 dB, respectively. Experimental limitations prevented us from verifying that the intermodulation distortion remains fifth-order limited at powers below the 10-kHz noise floor. Column 3 lists the calculated performance had the link achieved the shot-noise limit, had γ been the nominal 1/3 for $LiNbO_3$, and removing the excess RF loss.

TABLE I
MEASURED AND PROJECTED LINK PERFORMANCE

	Meas.	**Calc.**	$\gamma = 1/3$	**high-perf.**
V_π (Volts)	3.25	3.25	3.25	1
γ^{a}	1/4.25	1/4.25	1/3	1/3
$i_{DC}{}^{b}$(mA)	6	6	6	40
shot limit[c]	N	N	Y	Y
TM-only:				
gain (dB)	–15.0	–13.7	–7.7	19.0
IIP3 (dBm)	11.0	13.3	13.3	3.1
SDFR (dB/Hz$^{2/3}$)	100.7	103.1	110.4	116
Linearized:				
gain (dB)	–27.5	–26.7	–18.3	8.4
IIP5 (dBm)	16.0	18.5	17.0	6.8
SDFR (dB/Hz$^{4/5}$)	115	117.4	127.7	133.6

[a] γ is defined as the ratio $V_\pi^{(\mathrm{TM})}/V_\pi^{(\mathrm{TE})}$.
[b] Average dc photocurrent, per detector.
[c] Indicates whether the link is (projected to be) operating in the shot-noise limit. The first two columns were evaluated using the experimentally measured noise floor while the last two columns assume shot-noise limited performance.

As a further exercise, performance has also been calculated in column 4 for a link with state-of-the-art components such as those described in the introduction. Desired high-performance device characteristics include sufficiently narrow linewidth sources to ensure phase-to-intensity noise is below the shot noise limit, a modulator V_π of 1 V (and $\gamma = 1/3$), and balanced detectors (with internal 50 Ω resistors) capable of 40-mA dc current per detector. With this link, the linearized SFDR would improve to 133 dB/Hz$^{4/5}$ in the shot-noise limit.

V. CONCLUSION

We have developed the theory for, and experimentally shown, a linearized fiber optic link with a single commercial optical phase modulator. This link uses two different wavelengths, one on each polarization axis of the modulator, to create two copies of the same signal, modulated to different depths. These two copies are recombined in the proper ratio after detection to suppress the third-order term of the IMD.

The experimental results verify third-order suppression at least within a 10-kHz bandwidth, and demonstrated a 15-dB improvement in SFDR in agreement with theory, despite the noise floor being significantly above the shot-noise limit. We have also calculated the link's performance if state-of-the-art components were used, which shows a link like this would be capable of an SFDR near 133 dB/Hz.

REFERENCES

[1] J. D. McKinney, M. Godinez, V. Urick, S. Thaniyavarn, W. Charczenko, and K. J. Williams, "Sub-10-dB noise figure in a multiple-GHz analog optical link," *IEEE Photon. Technol. Lett.*, vol. 19, no. 7, pp. 465–467, 2007.

[2] E. I. Ackerman and C. H. Cox, "Microwave photonic links with gain and low noise figure," in *20th Annu. Meeting IEEE Lasers Electro-Optics Soc.*, Oct. 21–25, 2007, pp. 38–39.

[3] E. I. Ackerman, G. E. Betts, W. K. Burns, J. C. Campbell, C. H. Cox, N. Duan, J. L. Prince, M. D. Regan, and H. V. Roussell, "Signal-to-noise performance of two analog photonic links using different noise reduction techniques," in *Proc. IEEE/MTT-S Int. Microwave Symp.*, Jun. 3–8, 2007, pp. 51–54.

[4] B. H. Kolner and D. W. Dolfi, "Intermodulation distortion and compression in an integrated electroopics modulator," *Appl. Opt.*, vol. 26, no. 17, pp. 3676–3680, 1987.

[5] T. R. Clark and M. L. Dennis, "Coherent optical phase-modulation link," *IEEE Photon. Technol. Lett.*, vol. 19, no. 16, pp. 1206–1208, 2007.

[6] H.-F. Chou, A. Ramaswamy, D. Zibar, L. A. Johansson, J. E. Bowers, M. Rodwell, and L. Coldren, "Highly linear coherent receiver with feedback," *IEEE Photon. Technol. Lett.*, vol. 19, no. 12, pp. 940–942, 2007.

[7] R. F. Kalman, J. Fan, and L. Kazovsky, "Dynamic range of coherent analog fiber-optic links," *J. Lightw. Technol.*, vol. 12, no. 7, pp. 1263–1277, Jul. 1994.

[8] M. J. LaGasse and S. Thaniyvarn, "Bias-free high-dynamic range phase-modulated fiber-optic link," *IEEE Photon. Technol. Lett.*, vol. 9, no. 5, pp. 681–683, 1997.

[9] V. Urick, F. Bucholtz, P. Devgan, J. McKinney, and K. Williams, "Phase modulation with interferometric detection as an alternative to intensity modulation with direct detection for analog-photonic links," *IEEE Trans. Microw. Theory Tech.*, vol. 55, no. 9, pp. 1978–1985, 2007.

[10] F. Bucholtz, V. J. Urick, and A. Campillo, "Comparison of crosstalk for amplitude and phase modulation in an analog fiber optic link," in *Proc. IEEE Int. Topical Meeting Microwave Photonics (MWP)*, 2004, pp. 66–69.

[11] G. Betts and F. O'Donnell, "Microwave analog optical links using suboctave linearized modulators," *IEEE Photon. Technol. Lett.*, vol. 8, no. 9, pp. 1273–1275, 1996.

[12] E. I. Ackerman, "Broad-band linearization of a Mach–Zehnder electrooptic modulator," *IEEE Trans. Microw. Theory Tech.*, vol. 47, no. 12, pp. 2271–2279, 1999.

[13] L. M. Johnson and H. V. Roussell, "Reduction of intermodulation distortion in interferometric optical modulators," *Opt. Lett.*, vol. 13, no. 10, pp. 928–930, 1988.

[14] L. M. Johnson and H. V. Roussell, "Linearization of an interferometric modulator at microwave ferquencies by polarization mixing," *IEEE Photon. Technol. Lett.*, vol. 2, no. 11, pp. 810–811, 1990.

[15] B. M. Haas and T. E. Murphy, "A simple, linearized, phase-modulated analog optical transmission system," *IEEE Photon. Technol. Lett.*, vol. 19, no. 10, pp. 729–731, 2007.

[16] B. M. Haas and T. E. Murphy, "Multi-octave microwave transmission over fiber with a single optical phase modulator," in *Proc. IEEE Avionics, Fiber-Optics, Photonics Technology Conf.*, 2007, pp. 11–12.

[17] A. Karim and J. Devenport, "Low noise figure microwave photonic link," in *Proc. IEEE/MTT-S Int. Microwave Symp.*, 2007, pp. 1519–1522.

[18] S. K. Korotky and R. M. Ridder, "Dual parallel modulation schemes for low-distortion analog optical transmission," *IEEE J. Sel. Areas Commun.*, vol. 8, no. 7, pp. 1377–1381, 1990.

[19] W. B. Bridges and J. H. Schaffner, "Distortion in linearized electrooptic modulators," *IEEE Trans. Microw. Theory Tech.*, vol. 43, no. 9, pp. 2184–2197, 1995.

[20] Y. L. M. R. Salehi and B. Cabon, "Signal and noise conversions in RF-modulated optical links," *IEEE Trans. Microw. Theory Tech.*, vol. 52, no. 4, pp. 1302–1309, 2004.

Bryan M. Haas (M'01) received the B.S. degree in physics from the U.S. Naval Academy, Annapolis, MD, in 1994 and the M.S. degree in electrical engineering from The Johns Hopkins University, Baltimore, MD, in 2001. He is currently working towards the Ph.D. degree in electrical engineering from the University of Maryland, College Park.

Upon graduating from the Naval Academy, he served as a Surface Warfare Officer in the U.S. Navy for seven years. He then worked at Corvis Corporation as a Product Development Engineer for ultra-long-haul optical transport systems. He is now a Research Engineer at the Laboratory for Physical Sciences, College Park, MD.

Vincent J. Urick (M'05) received the B.S. degree (*magna cum laude*) in physics with minors in electronics and mathematics from Bloomsburg University, Bloomsburg, PA, in 2001, and the M.S. and Ph.D. degrees in applied physics from George Mason University, Fairfax, VA, in 2005 and 2007, respectively.

In 2001, he joined the U.S. Naval Research Laboratory, Washington, DC, where he works as a Research Physicist in the Photonics Technology Branch, developing analog-photonic systems. His current research interests include HF/VHF and microwave and millimeter-wave applications of radio-frequency analog photonics.

Dr. Urick is a member of Sigma Pi Sigma and Phi Kappa Phi.

Jason D. McKinney (S'99–M'03) received the Ph.D. degree in electrical engineering from Purdue University, West Lafayette, IN, in 2003. His doctoral work included the first demonstration of ultrafast optical pulse-shaping techniques for synthesis of arbitrarily shaped millimeter waveforms exhibiting arbitrary phase and frequency modulation at center frequencies up to 50 GHz.

After completing the Ph.D. degree, he was a Visiting Assistant Professor from 2003 to 2005 and a Research Scientist from 2005 to 2006 in the School of Electrical and Computer Engineering at Purdue University. He is currently with the Microwave Photonics Section, Optical Sciences Division, of the U.S. Naval Research Laboratory, Washington, DC. His research interests include low-noise, high-power analog optical links, ultrafast optical pulse processing, and applications of photonics in ultrabroadband microwave systems. He has authored or coauthored over 14 journal articles, one book chapter, and over 27 conference papers

Dr. McKinney has received a variety of awards for his research, most notably, the Chorafas Prize for doctoral research in 2003 (awarded to one Purdue doctoral student per year) and as a finalist for the Optical Society of America (OSA)/New Focus Student Award (2002). He has also received numerous awards in recognition of his teaching and is an Associate Fellow of the Purdue University Teaching Academy. He is a member of the OSA.

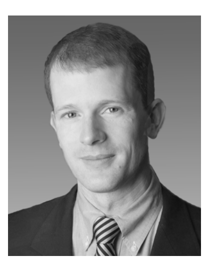

Thomas E. Murphy (M'94–SM'07) received the B.A. degree in physics and the B.S.E.E. degree in electrical engineering from Rice University, Houston, TX, in 1994 and the M.S. and Ph.D. degrees, both in electrical engineering, from the Massachusetts Institute of Technology, Cambridge, in 1994 and 1997, respectively.

In 1994, he joined the NanoStructures Laboratory at MIT, where he pursued research in integrated optics and nanotechnology. In 2000, he joined MIT Lincoln Laboratory, Lexington, MA, as a staff member in the Optical Communications Technology Group, where he studied and developed ultrafast optical communications systems. In August 2002, he joined the faculty at the University of Maryland, College Park, as an Assistant Professor in the Department of Electrical and Computer Engineering. His research interests include optical communications, short-pulse phenomena, numerical simulation, optical pulse propagation, nanotechnology and integrated photonics.

Dr. Murphy is a member of the Optical Society of America (OSA) and a recipient of the National Science Foundation (NSF) CAREER award.